

New Thiazolothiazole Copolymer Semiconductors for Highly Efficient Solar Cells

Selvam Subramaniyan, Hao Xin, Felix Sunjoo Kim, and Samson A. Jenekhe*

Department of Chemical Engineering and Department of Chemistry, University of Washington, Seattle, Washington 98195-1750, United States

S Supporting Information

1. INTRODUCTION

π -Conjugated polymer semiconductors with donor–acceptor (D–A) architectures are of growing interest in view of their applications in low-cost solar cells.^{1–4} D–A copolymers are advantageous because of the facile tunability of their absorption bands, charge carrier mobilities, and HOMO–LUMO levels, depending on the choice and strength of the electron-donating (D) and electron-withdrawing (A) segments.^{1–5} Among recent examples of D–A copolymers found to be good p-type semiconductors for developing highly efficient bulk heterojunction (BHJ) solar cells include those containing donor moieties such as benzodithiophene and dithienosilole and acceptors such as thieno(3,4-*b*)thiophene-2-carboxylate^{2a} and thieno(3,4-*c*)pyrrole-4,6-dione.^{2b,3b} p-Type polymer semiconductors with high carrier mobilities were recently developed from electron-deficient thiazolothiazole (TT) ring and used to realize high-performance field-effect transistors.⁶ TT-based copolymers were recently also demonstrated to be promising in bulk heterojunction (BHJ) solar cells, showing power conversion efficiency of 2–5%.⁷ There remains a need to explore new p-type polymer semiconductors with D/A combinations to further understand the underlying structure–property relationships and toward the discovery of design criteria of optimum materials for highly efficient solar cells. Among the specific aims in the design of new p-type polymers for high-performance polymer solar cells are to achieve low-lying HOMO levels (–5.2 to –5.7 eV) toward higher open-circuit voltage, small band gap (1.2–1.9 eV) for more efficient light harvesting, high charge carrier mobility ($>0.001 \text{ cm}^2/(\text{V s})$), optimal solid-state morphology, and HOMO/LUMO levels well matched to the fullerene acceptors for more efficient charge separation.

We report herein new thiazolothiazole-based D–A copolymers PTBSTT and PSDTTT (Chart 1) that combine small band gaps (1.73–1.77 eV), broad absorption band, high carrier mobility, and oxidative stability with excellent film forming properties. These copolymers were enabled by the design and synthesis of a novel monomer, 2,5-bis(5-bromo-4,4'-dioctyl-dithieno[3,2-*b*:2',3'-*d*]silole)thiazolo[5,4-*d*]thiazole, in which the TT unit is flanked by dithienosilole moieties with the aim of improving oxidative stability, π -stacking, intramolecular charge-transfer interactions, crystallinity, and charge photogeneration and transport. In field-effect transistors, PTBSTT and PSDTTT showed p-channel characteristics and average mobility of 0.009–0.042 $\text{cm}^2/(\text{V s})$ with high on/off current ratios ($>10^5$ – 10^6). Bulk heterojunction (BHJ) solar cells incorporating

the new copolymer PSDTTT as a donor with [6,6]-phenyl C₇₁-butyric acid methyl ester (PC₇₁BM) acceptor had an average power conversion efficiency of 5.3% under 100 mW/cm² AM1.5G irradiation in air.

2. EXPERIMENTAL SECTION

Experimental details of the synthesis of monomers **5**, **8**, and **9** and the polymer PTBSTT can be found in the Supporting Information. Poly[(4,8-di(2-butyloctyloxy)benzo[1,2-*b*;4,4'-*b*]dithiophene)-2,6'-diyl-*alt*-(2,5-bis(4,4'-bis(2-octyl)dithieno[3,2-*b*:2',3'-*d*]silole-2,6-diyl)thiazolo[4,4-*d*]thiazole)] (PSDTTT): The distannyl compound **8** (260 mg, 0.30 mmol) and dibromo compound **5** (330 mg, 0.30 mmol) and catalyst tris(dibenzylideneacetone)dipalladium (0) (5 mg, 0.06 mmol) and tri-*o*-tolylphosphine (7 mg, 0.2 mmol) in anhydrous chlorobenzene (23 mL) were heated at 80 °C for 36 h. The temperature was then reduced to 50 °C. The reaction mixture was poured into 200 mL of methanol containing 5 mL of hydrochloric acid and stirred for 5 h. The brown precipitate was collected via filtration and was further purified by Soxhlet extraction with methanol and hexane. The remaining solid obtained was dried under vacuum to afford PSDTTT in 90% yield. GPC: M_n = 13.1 kDa, PDI = 3.39. ¹H NMR (CDCl₃, 300 MHz, ppm): δ 0.88–2.15 (m, 106 H), 2.55–2.88 (m, 8H), 3.82–4.11 (m, br, 4H), 6.2–6.8 (m, br, 6H).

3. RESULTS AND DISCUSSION

3.1. Synthesis. PTBSTT and PSDTTT were synthesized by Stille-type copolymerization of a new dibromide **5** with the distannyl compounds **9** and **8**, respectively, in anhydrous chlorobenzene (Scheme 1). The new comonomer **5** was synthesized in four steps from 3,3'-dibromo-2,2'-bithiophene (**1**). Vilsmeier formylation of **2** yielded the corresponding aldehyde **3**, which was converted into thiazolothiazole derivative **4** in 20% yield. Treatment of thiazolothiazole compound **4** with NBS in chloroform/acetic acid (2:1) gave the dibromide **5** as a red solid in 80% yield (Scheme 1). The comonomer **8** was synthesized from compound **6** in two steps. Further details of the synthesis and characterization of the monomers are given in the Supporting Information. PSDTTT was readily soluble in organic solvents

Received: May 8, 2011

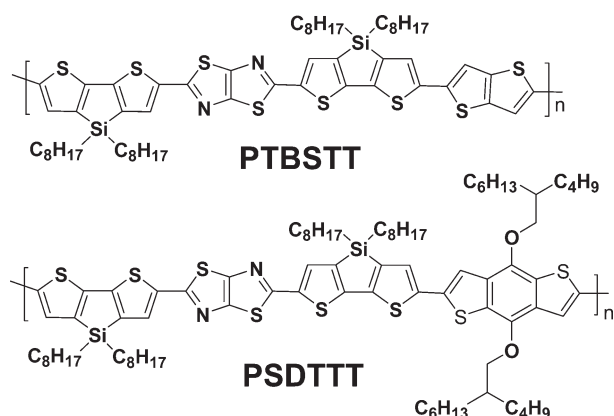
Revised: July 15, 2011

Published: July 25, 2011

(chloroform, chlorobenzene, 1,2-dichlorobenzene, etc.) at room temperature, whereas PTBSTT was less soluble in these solvents even at higher temperatures ($>100\text{ }^{\circ}\text{C}$). PSDTTT had moderate number-average molecular weight of 13.1 kDa with a polydispersity index of 3.39.

3.2. Optical and Electrochemical Properties. The solution and thin film absorption spectra of the new copolymers are shown in Figure 1. In dilute solution (10^{-6} M), PTBSTT and

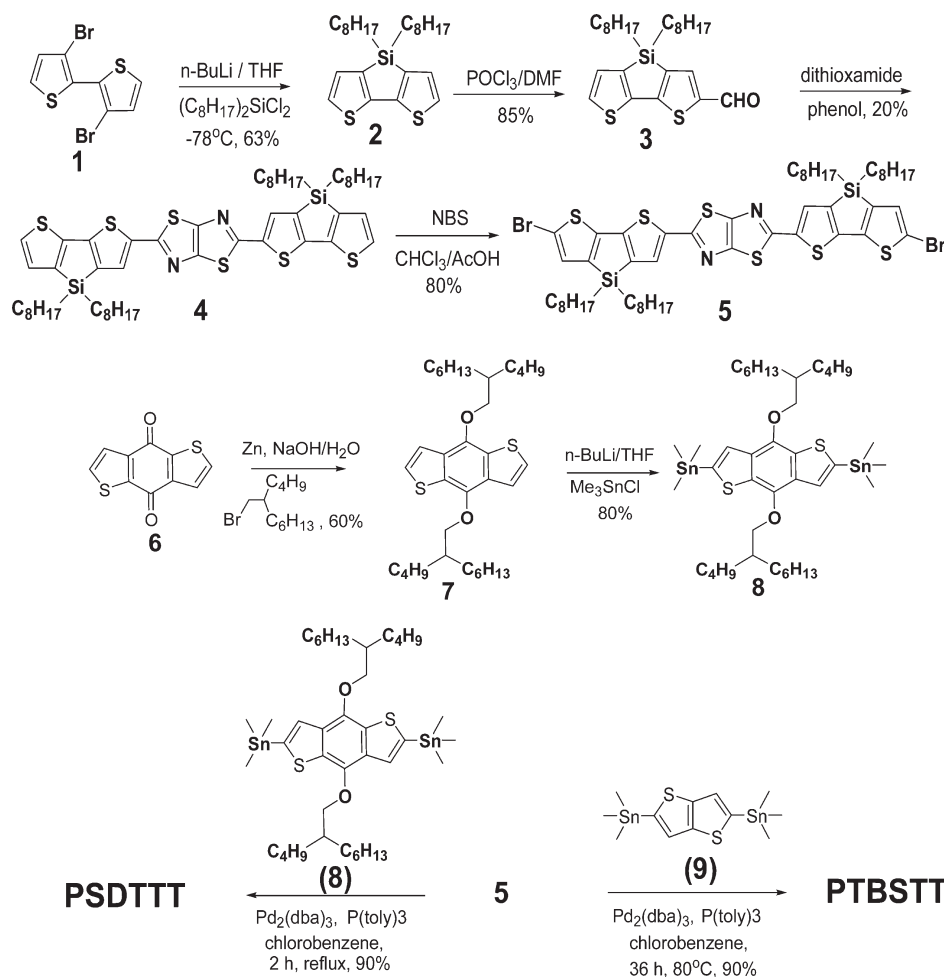
Chart 1. Molecular Structures of New Thiazolothiazole-Based Copolymers



PSDTTT have identical absorption spectra with an absorption maximum at 572–574 nm (Figure 1a). The thin film absorption spectrum of PSDTTT has a vibronic structure with a peak at 576 nm and a shoulder at 614 nm, resulting in an absorption edge optical band gap (E_g^{opt}) of 1.77 eV. The thin film absorption spectrum of the thienothiophene-linked polymer PTBSTT also has a vibronic structure but is slightly red-shifted from that of PSDTTT (Figure 1b), giving a lower energy maximum at 649 nm and a higher energy vibronic peak at 604 nm. The optical band gap of PTBSTT at 1.73 eV is slightly reduced compared to PSDTTT. The resolved vibronic structure of the absorption spectra of both polymer thin films suggest that the polymer chains are relatively planar with strong intramolecular order in the solid state.⁸ The HOMO/LUMO energy levels of PTBSTT and PSDTTT, estimated from cyclic voltammetry (Supporting Information, Figure S1),⁹ were $-5.3/-3.7\text{ eV}$ and $-5.4/-3.6\text{ eV}$, respectively.

3.3. Morphology and Molecular Packing. X-ray diffraction (XRD) studies on drop-casted thin films on ITO-coated glass substrates (annealed at $150\text{ }^{\circ}\text{C}$ for 20 min) were carried out to investigate the solid-state morphology and molecular packing of PTBSTT and PSDTTT. Figure 2 shows the XRD patterns of the polymer films. Strong and weak peaks corresponding to (100) and (200) reflections, respectively, are observed in the XRD patterns of PTBSTT film, indicating a high degree of crystallinity in the PTBSTT thin films. The (100) lamellar reflection corresponds to

Scheme 1. Synthetic Route to PTBSTT and PSDTTT



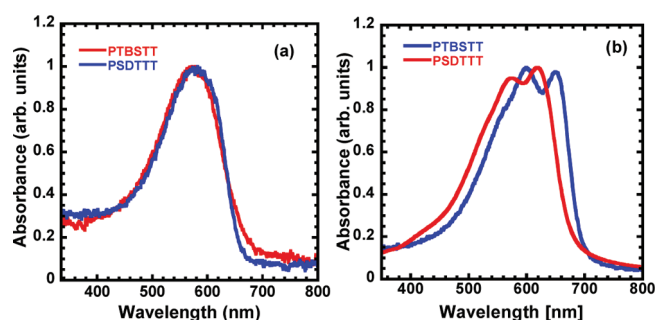


Figure 1. Absorption spectra of PTBSTT and PSDTTT: (a) in dilute 1,2-dichlorobenzene solutions and (b) as thin films.

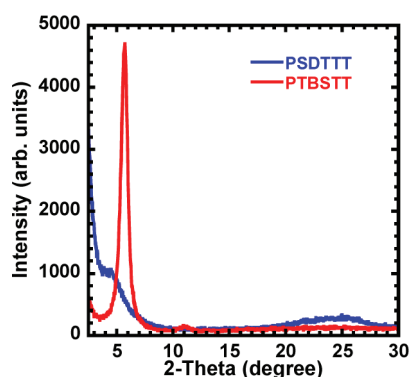


Figure 2. X-ray diffraction spectra of PSDTTT and PTBSTT thin films.

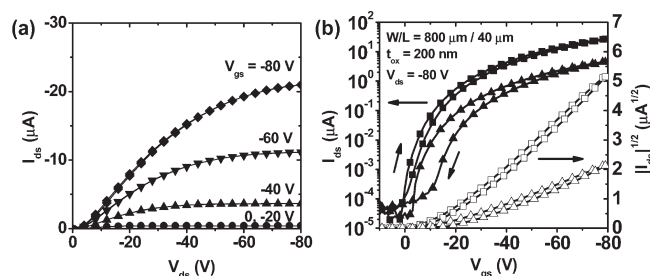


Figure 3. (a) Output curves of a PTBSTT FET and (b) overlays of transfer characteristics of PTBSTT (square) and PSDTTT (triangle) FETs. Forward and backward scans are overlaid in both panels.

d -spacing of 1.56 nm. The absence of a π - π stacking diffraction indicates that most of the PTBSTT polymer chains predominantly adopts a layered structure with an edge-on orientation relative to the substrate,^{10a,11} which is similar to reported XRD results for other dithienosilole-based polymer semiconductors.^{10b} In contrast, PSDTTT films showed a very weak diffraction peak at 2.13 nm, suggesting that this polymer is largely amorphous and similar to other thiazolothiazole polymers.⁶

3.4. Field Effect Transistors (FETs). The output and transfer characteristics of field-effect transistors fabricated from PTBSTT as well as the transfer characteristics of PSDTTT OFETs are shown in Figure 3. Both polymers showed typical p-channel characteristics with a good current modulation with on/off current ratios ($I_{\text{on}}/I_{\text{off}}$) higher than 10^5 . PTBSTT had an average hole mobility of $0.042 \pm 0.006 \text{ cm}^2/(\text{V s})$. A small hysteresis between the forward and backward scans was observed in both output and transfer curves of PTBSTT devices. PSDTTT also

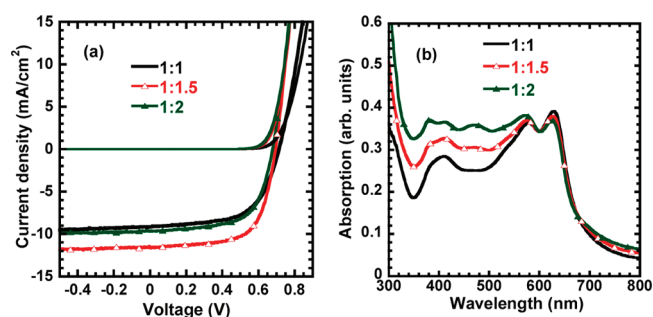


Figure 4. (a) Current density–voltage characteristics of PSDTTT:PC₇₁BM (1:1, 1:1.5, and 1:2) solar cells with a structure of ITO/PEDOT/PSDTTT:PC₇₁BM/LiF/Al under dark and 100 mW/cm² 1.5AM sunlight illumination. (b) Absorption spectra of the same devices as in (a).

Table 1. Photovoltaic Parameters of PSDTTT:PC₇₁BM Solar Cells

PSDTTT:PC ₇₁ BM	J_{sc} (mA/cm ²)	V_{oc} (V)	FF	η_{ave} (%)
1:1	9.17	0.71	0.60	3.9 ± 0.1
1:1.5	11.6	0.69	0.66	5.3 ± 0.1
1:2	9.70	0.67	0.64	4.1 ± 0.1

showed a good current modulation and saturation and had a lower average mobility of $0.009 \pm 0.001 \text{ cm}^2/(\text{V s})$ (Supporting Information, Figure S2). Threshold voltages were -10.4 V for PTBSTT and -19.7 V for PSDTTT. Although the greater lamellar crystalline order in PTBSTT films, as observed in the above XRD results, may appear to explain its factor of 4.67 greater carrier mobility, we note that hole mobilities as high as $0.30 \text{ cm}^2/(\text{V s})$ have been observed in other amorphous thiazolothiazole copolymers.^{6b} We also note that despite the relatively low-lying LUMO energy levels of -3.6 and -3.7 eV , we have not observed electron transport properties from any of these two polymer semiconductors as would be expected if they were ambipolar.^{5c,d}

3.5. Photovoltaic Cells. The photovoltaic properties of the new copolymer PSDTTT were investigated in BHJ solar cells using PC₇₁BM as the acceptor. Three different compositions of the active layer, PSDTTT:PC₇₁BM = 1:1, 1:1.5, and 1:2, were investigated. The current density–voltage (J – V) curves of the solar cells are shown in Figure 4a. The best solar cell performance was achieved in PSDTTT:PC₇₁BM (1:1.5) blend film with an average power conversion efficiency of 5.3%. The current density (J_{sc}), open-circuit voltage (V_{oc}), and fill factor (FF) measured in this solar cell are 11.6 mA/cm^2 , 0.69 V , and 0.66 , respectively (Table 1). The performance decreased significantly on either side of the 1:1.5 composition, suggesting that this is the optimum composition for this polymer. The absorption spectra of all the blend films shown in Figure 4b have similar absorption features with characteristic peaks at 575 and 625 nm, which are identical to the pure PSDTTT film (Figure 1b). The obvious absorption enhancement in the 350–550 nm wavelength range with higher PC₇₁BM loading is observed. The best photovoltaic performance of PSDTTT:PC₇₁BM solar cells comes from the 1:1.5 ratio at which the various parameters are maximized, especially the current density and fill factor (Table 1). The external quantum efficiency (EQE) spectrum of the best PSDTTT:PC₇₁BM (1:1.5) solar cell is shown in Figure 5. This device has a high photoconversion efficiency with EQE greater than 50% in the

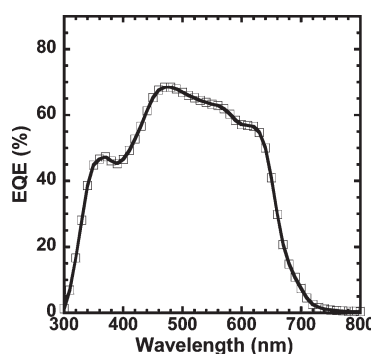


Figure 5. EQE spectrum of PSDTTT:PC₇₁BM (1:1.5) solar cells.

wavelength range of 410–640 nm and a peak value of 68.5% at 480 nm. A mismatch factor of 5% was observed between the J_{sc} calculated by integrating the EQE curve with an AM1.5G reference spectrum and that from the J – V measurements.

Because of the poor solubility of PTBSTT and consequent large polymer aggregates formed during spin-coating of PTBSTT:PC₇₁BM blend films, the efficiency of devices made from this polymer was significantly lower. The photovoltaic efficiency of PTBSTT:PC₇₁BM (1:2) solar cells was only 0.97% PCE with a J_{sc} , V_{oc} , and FF of 2.73 mA/cm², 0.64 V, and 0.56, respectively. However, on the basis of high hole mobility, crystallinity, and relatively red-shifted absorption of PTBSTT compared to PSDTTT, we expect that better photovoltaic devices could be developed from PTBSTT-type materials by improving the polymer solubility.

4. CONCLUSIONS

Stille-type copolymerization of the novel monomer, 2,5-bis(5-bromo-4,4'-diocetyl-dithieno[3,2-*b*:2',3'-*d'*]silole)-thiazolo[5,4-*d*]-thiazole, has produced new thiazolothiazole-based copolymer semiconductors found to have promising charge transport and photovoltaic properties. PTBSTT and PSDTTT had hole mobilities of 0.009–0.042 cm²/(V s). The slightly higher hole mobility of PTBSTT was attributed to the high crystallinity of the polymer thin film as observed from X-ray diffraction. PC₇₁BM-based BHJ solar cells utilizing PSDTTT were found to have a power conversion efficiency of 5.3% under one sun AM 1.5G illumination. These results demonstrate that high-efficiency (>5%) solar cells can be achieved from the new thiazolothiazole-based copolymer semiconductors.

■ ASSOCIATED CONTENT

Supporting Information. Experimental details on syntheses and characterization of monomers, cyclic voltammetry, and device fabrication and testing. This material is available free of charge via the Internet at <http://pubs.acs.org>.

■ AUTHOR INFORMATION

Corresponding Author

*E-mail: jenekhe@u.washington.edu.

■ ACKNOWLEDGMENT

Our report is based on research (excitonic solar cells) supported by the U.S. Department of Energy, Office of Basic Energy

Sciences, Division of Material Sciences, under Award DE-FG02-07ER46467. The NSF (DMR-0805259 and DMR-0120967) supported the synthesis and field-effect charge transport properties of the donor–acceptor copolymers.

■ REFERENCES

- (1) Recent reviews: (a) Cheng, Y.-J.; Yang, S.-H.; Hsu, C.-S. *Chem. Rev.* **2009**, *109*, 5868–5923. (b) Thompson, B. C.; Fréchet, J. M. J. *Angew. Chem., Int. Ed.* **2008**, *47*, 58–77. (c) Boudreault, P. T.; Najari, A.; Leclerc, M. *Chem. Mater.* **2011**, *23*, 456–469. (d) Kim, F. S.; Ren, G.; Jenekhe, S. A. *Chem. Mater.* **2011**, *23*, 682–732.
- (2) (a) Liang, Y.; Xu, Z.; Xia, J.; Tsai, S.-T.; Wu, Y.; Li, G.; Ray, C.; Yu, L. *Adv. Mater.* **2010**, *22*, E135–E138. (b) Piliago, C.; Holcombe, T. W.; Douglas, J. D.; Woo, C. H.; Beaujuge, P. M.; Fréchet, J. M. J. *J. Am. Chem. Soc.* **2010**, *132*, 7595–7597. (c) Wang, E.; Hou, E.; Wang, E.; Hellström, E.; Zhan, F.; Inganäs, O.; Andersson, M. R. *Adv. Mater.* **2010**, *22*, S240–S244.
- (3) (a) Bronstein, H.; Chen, Z.; Ashraf, R. S.; Zhang, W.; Du, J.; Durrant, J. R.; Tuladhar, P. S.; Song, K.; Watkins, S. E.; Geerts, Y.; Wienk, M. M.; Janssen, R. A. J.; Anthopoulos, T.; Sirringhaus, H.; Heeney, M.; McCulloch, M. J. *Am. Chem. Soc.* **2011**, *133*, 3272–3275. (b) Chu, T.; Lu, J.; Beaupre, S.; Zhang, Y.; Pouliot, J.; Wakim, S.; Zhou, J.; Leclerc, M.; Li, Z.; Ding, J.; Tao, Y. *J. Am. Chem. Soc.* **2011**, *133*, 4250–4253. (c) Zhou, H.; Yang, L.; Stuart, A. C.; Price, S. C.; Liu, S.; You, W. *Angew. Chem., Int. Ed.* **2011**, *50*, 2995–2998.
- (4) (a) Wu, P.-T.; Bull, T.; Kim, F. S.; Luscombe, C. K.; Jenekhe, S. A. *Macromolecules* **2009**, *42*, 671–681. (b) Ahmed, E.; Kim, F. S.; Xin, H.; Jenekhe, S. A. *Macromolecules* **2009**, *42*, 8615–8618. (c) Guo, X.; Xin, H.; Kim, F. S.; Liyanage, A. D. T.; Jenekhe, S. A.; Watson, M. D. *Macromolecules* **2011**, *44*, 269–277. (d) Xin, H.; Kim, F. S.; Jenekhe, S. A. *J. Am. Chem. Soc.* **2008**, *130*, 5424–5425.
- (5) (a) Guo, X.; Kim, F. S.; Jenekhe, S. A.; Watson, M. D. *J. Am. Chem. Soc.* **2009**, *131*, 7206–7207. (b) Beaujuge, P. M.; Pisula, W.; Tsao, H. N.; Ellinger, S.; Mullen, K.; Reynolds, J. R. *J. Am. Chem. Soc.* **2009**, *131*, 7514–7515. (c) Kim, F. S.; Guo, X.; Watson, M. D.; Jenekhe, S. A. *Adv. Mater.* **2010**, *22*, 478–482. (d) Babel, A.; Zhu, Y.; Cheng, K. F.; Chen, W. C.; Jenekhe, S. A. *Adv. Funct. Mater.* **2007**, *17*, 2542–2549.
- (6) (a) Osaka, I.; Sauvé, G.; Zhang, R.; Kowalewski, T.; McCullough, R. D. *Adv. Mater.* **2007**, *19*, 4160–4165. (b) Osaka, I.; Zhang, R.; Sauvé, G.; Smilgies, D.-M.; Kowalewski, T.; McCullough, R. D. *J. Am. Chem. Soc.* **2009**, *131*, 2521–2529.
- (7) (a) Subramaniam, S.; Xin, H.; Kim, F. S.; Shoaee, S.; Durrant, J. R.; Jenekhe, S. A. *Adv. Energy Mater.* **2011**, DOI 10.1002/aenm.201100215. (b) Jenekhe, S. A.; Subramaniam, S.; Xin, H.; Kim, F. International Patent Application No. PCT/EP2010/066179, Oct 26, 2010. (c) Jung, I. H.; Yu, J.; Jeong, E.; Kim, J.; Kwon, S.; Kong, H.; Lee, K.; Woo, H. Y.; Shim, H. K. *Chem.—Eur. J.* **2010**, *16*, 3743–3752. (d) Lee, S. K.; Cho, J. M.; Goo, Y.; Shin, W. S.; Lee, J.; Lee, W.; Kang, I.; Shim, H.; Moon, S. *Chem. Commun.* **2011**, *47*, 1791–1793.
- (8) Osaheni, J. A.; Jenekhe, S. A. *Chem. Mater.* **1992**, *4*, 1282–1290.
- (9) Agrawal, A. K.; Jenekhe, S. A. *Chem. Mater.* **1996**, *8*, 579–589.
- (10) (a) McCulloch, I.; Heeney, M.; Bailey, C.; Genevicius, K.; MacDonald, I.; Shkunov, M.; Sparrowe, D.; Tierney, S.; Wagner, R.; Zhang, W.; Chabinyc, M. L.; Kline, R. J.; McGehee, M. D.; Toney, M. F. *Nature Mater.* **2006**, *5*, 328–333. (b) Lu, G.; Usta, H.; Risko, C.; Wang, L.; Facchetti, A.; Ratner, M. A.; Marks, T. J. *J. Am. Chem. Soc.* **2008**, *130*, 7670–7685.
- (11) Sirringhaus, H.; Brown, P. J.; Friend, R. H.; Nielsen, M. M.; Bechgaard, K.; Langeveld-Voss, B. M. W.; Spiering, A. J. H.; Janssen, R. A. J.; Meijer, E. W.; Herwig, P.; de Leeuw, D. M. *Nature* **1999**, *401*, 685–688.